

Rozeni Chagas Lima Teles,<sup>a</sup>  
Gisele Ferreira Esteves,<sup>a</sup>  
Marcus Aurélio Miranda Araújo,<sup>a</sup>  
Carlos Bloch Jr,<sup>b</sup>  
João Alexandre Ribeiro  
Gonçalves Barbosa<sup>c\*</sup> and  
Sonia Maria de Freitas<sup>a\*</sup>

<sup>a</sup>Laboratório de Biofísica, Instituto de Ciências Biológicas, Universidade de Brasília, Brasília-DF, 70910-900, Brazil, <sup>b</sup>Laboratório de Espectrometria de Massa, Empresa Brasileira de Pesquisa Agropecuária – Recursos Genéticos e Biotecnologia, Brasília-DF, 70770-900, Brazil, and <sup>c</sup>Center for Structural Molecular Biology (CeBiME), Brazilian Synchrotron Light Laboratory (LNLS), CP-6192, Campinas-SP, 13084-971, Brazil

Correspondence e-mail: joao@lnls.br,  
nina@unb.br

Received 8 August 2007  
Accepted 15 September 2007

## Crystallization and preliminary crystallographic studies of *Schizolobium parahyba* chymotrypsin inhibitor (SPCI) at 1.8 Å resolution

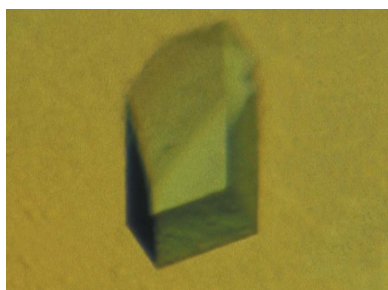
SPCI, a Kunitz-type chymotrypsin inhibitor, is a 180-amino-acid polypeptide isolated from *Schizolobium parahyba* seeds. This inhibitor has been characterized as a highly stable protein over a broad pH and temperature range. SPCI was crystallized using a solution containing 0.1 M sodium acetate trihydrate buffer pH 4.6, 33% (v/v) PEG 2000 and 0.2 M ammonium sulfate. Data were collected to 1.80 Å resolution from a single crystal of SPCI under cryogenic conditions. The protein crystallized in space group  $P2_12_12$ , with unit-cell parameters  $a = 40.01$ ,  $b = 71.58$ ,  $c = 108.68$  Å and an  $R_{\text{merge}}$  of 0.052. The structure of SPCI has been solved by molecular replacement using the known structure of the Kunitz-type trypsin inhibitor from *Delonix regia* (PDB code 1r8n) as the search model.

### 1. Introduction

Proteinase inhibitors are widely distributed in animals, plants and microorganisms, in which they act as antinutritional agents, and particularly in insects, in which they inhibit midgut proteases. They also inhibit a broad spectrum of activities including the suppression of pathogenic nematodes and the growth inhibition of many pathogenic fungi (Joshi *et al.*, 1998). These inhibitors are divided into synthetic and natural inhibitors and 18 different families have been classified (Laskowski & Qasim, 2000). The representative members of these families mainly differ in molecular weight, disulfide-bond content, specificity, three-dimensional structure and stability to heat and to denaturing agents. Two main inhibitor families from leguminous plants have been characterized and are known as Kunitz-type and Bowman–Birk-type proteinase inhibitors (Laskowski & Kato, 1980; Valueva & Mosolov, 1999). The Kunitz-type inhibitors are divided into two subfamilies consisting of the bovine pancreatic trypsin inhibitor (BPTI) and soybean trypsin inhibitor (STI) subfamilies, represented by proteins with a molecular weight of about 6.5 kDa and three disulfide bonds and proteins with a molecular weight of about 20 kDa and two disulfide bonds, respectively.

Kunitz-type inhibitors have been reported to have the potential to suppress ovarian cancer cell invasion and peritoneal disseminated metastasis *in vivo* (Kobayashi *et al.*, 2004) and to have an adverse effect on insect development (Shukle & Wu, 2003). Furthermore, the complexes of the natural protein inhibitors with serine proteinases of the chymotrypsin and subtilisin families are among the most widely studied models of protein–protein recognition (Otlewski *et al.*, 1999; Ascenzi *et al.*, 2003). These advantages make proteinase inhibitors an ideal choice for use in medicine and agricultural biotechnological applications, especially in the development of transgenic crops that are resistant to insect pests. In this context, knowledge of their structural features is fundamental in order to understand the inhibitor–enzyme interactions and to allow novel approaches in the use of synthetic inhibitors with the aim of drug design.

*Schizolobium parahyba* chymotrypsin inhibitor (SPCI) is a STI-subfamily Kunitz-type inhibitor with a single polypeptide chain, presenting four cysteine residues linked into two disulfide bonds (Souza *et al.*, 1995; Teles *et al.*, 2004). It suppresses the proteolytic activity of chymotrypsin through the formation of a stable complex



© 2007 International Union of Crystallography  
All rights reserved

with a 1:1 stoichiometry. Thermodynamic analysis using spectroscopic and calorimetric methods reveals that SPCI is a thermally stable protein over the wide pH range from 3.0 to 8.8 and that it exhibits high stability in the pH range 5.0–7.0 (Teles *et al.*, 2005). The secondary structure of SPCI is mainly formed of  $\beta$ -strands (Teles *et al.*, 1999) and its native structure is mainly maintained by hydrophobic forces and electrostatic interactions (Souza *et al.*, 2000). The molecular arrangements of SPCI at pH 7.0, visualized by atomic force microscopy at high resolution in nanopure water, indicated organization into different oligomeric states, with a predominance of hexagonal forms (Leite *et al.*, 2002). In this work, we present the crystallization, data collection and phasing of the three-dimensional structure of SPCI in the dimeric state at 1.80 Å resolution.

## 2. Material and methods

### 2.1. Purification of SPCI

SPCI was purified following trichloroacetic acid (TCA) precipitation and ion-exchange chromatography (Teles *et al.*, 2004). Briefly, proteins from a crude extract were precipitated with 0.5–1.5% (w/v) TCA for 5 min in an Omnimixer homogenizer at medium speed. After centrifugation at 13 000g for 30 min, the supernatant was dialyzed against water at 277 K, lyophilized and dissolved in 50 mM acetate buffer pH 3.2. The soluble protein fraction was applied onto a SP-Sephadex C 25-120 column (2 × 15 cm) equilibrated with 50 mM acetate buffer pH 3.2. The inhibitor was eluted with a linear salt gradient from 0.2 to 1.0 M NaCl in the same buffer.

### 2.2. Crystallization and data processing

SPCI was crystallized using the sitting-drop vapour-diffusion method (McPherson, 1990) at 294 K. Initial crystallization trials were performed using the commercial screens Crystal Screen and Crystal Screen II from Hampton Research. The reservoir contained 300  $\mu$ l solution and the drops were prepared by adding 2  $\mu$ l reservoir solution to 2  $\mu$ l protein solution (lyophilized protein dissolved in Milli-Q water) at a concentration of 12–20 mg ml<sup>-1</sup>. After screening and optimization of the crystallization conditions, the best crystals were grown using the same drop and reservoir volumes with protein dissolved in water at 20 mg ml<sup>-1</sup> and precipitant consisting of 0.1 M

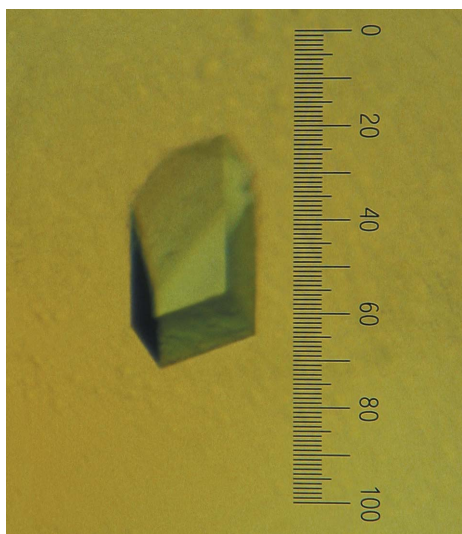


**Figure 1**  
A crystal of SPCI grown by the vapour-diffusion method at 294 K.

**Table 1**

Data-collection and processing statistics for the SPCI crystal.

Values in parentheses are for the highest resolution shell.

|                                   |                                    |
|-----------------------------------|------------------------------------|
| Space group                       | $P2_12_12$                         |
| Unit-cell parameters (Å)          | $a = 40.01, b = 71.58, c = 108.68$ |
| Mosaicity (°)                     | 0.4                                |
| Temperature (K)                   | 100                                |
| Wavelength (Å)                    | 1.421                              |
| Oscillation (°)                   | 1.0                                |
| Crystal-to-detector distance (mm) | 70.0                               |
| No. of frames                     | 152                                |
| Resolution limits (Å)             | 40.00–1.80 (1.86–1.80)             |
| $I/\sigma(I)$ after merging       | 32.7 (5.1)                         |
| Completeness (%)                  | 99.8 (99.5)                        |
| Multiplicity                      | 5.8 (5.5)                          |
| $R_{\text{merge}}^{\dagger}$      | 0.052 (0.369)                      |
| No. of reflections                | 171977                             |
| No. of unique reflections         | 29696 (2922)                       |

$\dagger R_{\text{merge}} = \sum_h \sum_i |I(h)_i - \langle I(h) \rangle| / \sum_h \sum_i I(h)_i$ , where  $I(h)$  is the intensity of reflection  $h$ ,  $\sum_h$  is the sum over all reflections and  $\sum_i$  is the sum over  $i$  measurements of reflection  $h$ .

sodium acetate trihydrate buffer pH 4.6, 33% (v/v) PEG 2000 and 0.2 M ammonium sulfate. Crystals were soaked in reservoir solution containing 15% (v/v) glycerol as a cryoprotectant for less than 30 s and mounted in a loop. The data were collected at the D03B-MX1 beamline of the Brazilian Synchrotron Light Laboratory (LNLS; Campinas, Brazil) at a wavelength of 1.431 Å with an oscillation of 1° on a MAR CCD detector with a circular X-ray-sensitive surface of 165 mm in diameter combined with a MAR DTB goniostat. Crystals were cryocooled in a stream of nitrogen gas at 110 K in order to minimize radiation damage. Data processing was performed with HKL-2000 (Otwinowski & Minor, 1997).

### 2.3. Molecular replacement

The Matthews coefficient was calculated using 20 460 Da as the molecular weight of the SPCI in order to indicate the number of molecules per asymmetric unit. The molecular-replacement solution for a dimer in the asymmetric unit was found using the crystallographic structure of the *Delonix regia* Kunitz-type trypsin inhibitor (Krauchenco *et al.*, 2003) as a search model. This procedure was performed using the MOLREP program (Vagin & Teplyakov, 1997) from the CCP4 package (Collaborative Computational Project, Number 4, 1994). The initial model had its side chains changed to correspond to the *S. parahyba* sequence using the graphics modelling package O (Jones *et al.*, 1991) and the temperature factors were set to 20.00 Å<sup>2</sup>.

## 3. Results and discussion

SPCI was purified from the crude extract by a precipitation step with 1.0% TCA, followed by ion-exchange chromatography (Teles *et al.*, 2004). SPCI at a concentration of 20 mg ml<sup>-1</sup> was crystallized using the vapour-diffusion method at 294 K. Crystals grew using a solution containing 0.1 M sodium acetate trihydrate buffer pH 4.6, 33% (v/v) PEG 2000 and 0.2 M ammonium sulfate (Fig. 1) and the largest crystals measured about 100 × 100 × 125  $\mu$ m. After data collection and processing, the crystals were found to belong to space group  $P2_12_12$ . Data in the resolution range 40.00–1.80 Å were obtained with an overall  $R_{\text{merge}}$  of 0.052, a completeness of 99.8% and an  $I/\sigma(I)$  of 32.7. Details of data-collection and processing statistics are presented in Table 1. Given an approximate molecular weight of 20 460 Da and the unit-cell parameters, the Matthews coefficients (Matthews, 1968) for one and two SPCI molecules per asymmetric unit were 3.8 and

$1.9 \text{ \AA}^3 \text{ Da}^{-1}$ , respectively. These values correspond to solvent contents of 67.4 and 34.8%, respectively.

The molecular-replacement protocol using the structure of the *D. regia* Kunitz-type trypsin inhibitor (Krauchenco *et al.*, 2003) as a search model yielded rotation-function and translation-function peaks that clearly corresponded to two molecules in the asymmetric unit.

This work was supported in part by Conselho Nacional de Desenvolvimento Científico e Tecnológico (CNPq), Coordenação de Aperfeiçoamento de Pessoal de Nível Superior (CAPES), Fundação de Amparo à Pesquisa do Estado de São Paulo (FAPESP) and Associação Brasileira de Tecnologia de Luz Síncrotron (ABTLuS).

## References

- Ascenzi, P., Bocedi, A., Bolognesi, M., Spallarossa, A., Colleta, M., De Cristofaro, R. & Menegatti, E. (2003). *Curr. Protein Pept. Sci.* **4**, 231–251.
- Collaborative Computational Project, Number 4 (1994). *Acta Cryst.* **D50**, 760–763.
- Jones, T. A., Zou, J.-Y., Cowan, S. W. & Kjeldgaard, M. (1991). *Acta Cryst.* **A47**, 110–119.
- Joshi, B., Sainani, M., Bastawade, K., Gupta, V. S. & Ranjekar, P. K. (1998). *Biochem. Biophys. Res. Commun.* **246**, 382–387.
- Kobayashi, H., Suzuki, M., Kanyama, N. & Terao, T. (2004). *Clin. Exp. Metastasis*, **21**, 159–166.
- Krauchenco, S., Pando, S. C., Marangoni, S. & Polikarpov, I. (2003). *Biochem. Biophys. Res. Commun.* **312**, 1303–1308.
- Laskowski, M. Jr & Kato, I. (1980). *Annu. Rev. Biochem.* **49**, 593–626.
- Laskowski, M. & Qasim, M. A. (2000). *Biochim. Biophys. Acta*, **1477**, 324–337.
- Leite, J. R. S. A., Silva, L. P., Taveira, C. C., Teles, R. C. L., Freitas, S. M. & Azevedo, R. B. (2002). *Protein Pept. Lett.* **9**, 179–185.
- McPherson, A. (1990). *Eur. J. Biochem.* **189**, 1–23.
- Matthews, B. W. (1968). *J. Mol. Biol.* **33**, 491–497.
- Otlewski, J., Krowarsch, D. & Apostoluk, W. (1999). *Acta Biochim. Pol.* **46**, 531–565.
- Otwinowski, Z. & Minor, W. (1997). *Methods Enzymol.* **276**, 307–326.
- Shukle, R. H. & Wu, L. (2003). *Environ. Entomol.* **32**, 488–498.
- Souza, E. M. T., Mizuta, K., Sampaio, M. U. & Sampaio, C. M. (1995). *Phytochemistry*, **39**, 521–525.
- Souza, E. M. T., Teles, R. C. L., Siqueira, E. M. A. & Freitas, S. M. (2000). *J. Protein Chem.* **19**, 507–513.
- Teles, R. C. L., Calderon, L. A., Medrano, F. J., Barbosa, J. A. R. G., Guimarães, B. G., Santoro, M. M. & Freitas, S. M. (2005). *Biophys. J.* **88**, 3509–3517.
- Teles, R. C. L., Freitas, S. M., Kawano, Y., Souza, E. M. T. & Áreas, E. P. G. (1999). *Spectrochim. Acta A*, **55**, 1279–1289.
- Teles, R. C. L., Souza, E. M. T., Calderon, L. A. & Freitas, S. M. (2004). *Phytochemistry*, **65**, 793–799.
- Vagin, A. & Teplyakov, A. (1997). *J. Appl. Cryst.* **30**, 1022–1025.
- Valueva, T. A. & Mosolov, V. V. (1999). *Russ. J. Plant Physiol.* **46**, 307–321.